Turkish Journal of Computer and Mathematics Education Vol.12 No.7 (2021), 2269-2287

ResearchArticle

A Novel Binary Texture Pattern's Based On Facial Expression Classification Using Neural Network

Regina Mathew Assistant professor[1*], Dr.M.S.Josephine professor [2], Dr.V.Jeyabalaraja professor [3]

[1]Dr.M.G.R Educational and Research Institute University Department of Computer application
reginamathew@loyolacollege.edu

[2]Dr.M.G.R Educational and Research Institute University Department of Computer application
josejbr@yahoo.com
[3]Velammal Engineering College Department of Computer science & Engineering
jeyabalaraja@gmail.com

Article History: Received: 11 January 2021; Revised: 12 February 2021; Accepted: 27 March 2021; Published online: 16 April 2021

Abstract:

The identification of facial expressions, due to its important academic and commercial ability, is an important topic in artificial intelligence. If we concentrate on the health care, it is an important goal of every healthcare service to identify and handle emotions of patients. Emotional health is important issues for human life. Bad emotions like depression, sad have influences in human life. To improve human social life, we need to identify their emotional conditions. Facial expressions are the most important means of discovering emotions and behavioral analysis. This paper presents framework for extracting the features by means of CS-LOP with gradient and Gabor wavelet feature and GLCM is designed for each method of feature extraction. Feature maps are fused and classified for different emotions.

Key Words: Feature extraction, facial expression recognition, CS-LOP, Neural Network, feature fusion

1. Introduction

Face is the human mind's index. The expression of the face shows the emotions and feelings of this assertion are common. An appearance that looks at one's face is known. Even after years of separation, recognition of identified individuals is made. Despite great improvements in visual stimulation due to viewing environments, expression, ageing and disturbances including glasses, the capacity is very robust. In the society of multimedia access to information, the identification of the face recently attracted much interest. Face recognition technology supports fields such as network protection, material indexing and recovery and video compression. It offers protection in the implementation of video and teleconferencing through its coding schemes. The management of network access through facial recognition practically renders it impossible for hackers to steal your password. Facial expression processing has also been a big influence for the research world over the last several decades, as it has a critical role in human-centered interfaces. In order to reach desired outcomes, certain technologies, including augmented reality, consumer profiling, video conferencing and client retention studies, need a strong degree of understanding of facial

expressions. Consequently, the influence of the identification of face expression on the above-mentioned applications is increasing continuously. Various efforts in facial expression recognition have been pursued. Psychologists identified the facial expressions under research as six important facial expressions (Disgust , anger, happiness, fear, surprise, and sadness) [2] [1], [3] [4], [6], [19].

1.1. Image Preprocessing

Several methods in image processing are also used to improve the image produced and to maximize popularity. De-nosing, Image normalization, filtering, histogram equalization, image resizing/cutting and effective facial detection are strategies for and improving recognition rate reinforcing the image standard. First as the input, the colour image is transformed into a grey image. The shot is then cut and the photo resized using an appropriate cropping approach. The picture is generic and structured. The picture is then screened using a low pass filter. Until the functionality is derived from the picture preprocessing is done [5].

1.1.1. Method for Face Detection and Cropping

Face detection is the method of identifying the applicant faces during the picture and deciding their positions. It's deemed a difficult activity because of the differences inside the pictures still because of the faces within them. The identification of faces such as scale, location, place, positions, expression and lighting conditions has several influences. Many face detection methods [20] are used in literature, several of them are computing-based approaches supported, and some are color-like extractions, and many approaches are backed by the principle of convergence. This paper aims to implement these forms of algorithms and incorporate them, such that improved outcomes are obtained. The Viola and Jones algorithm is currently the most common and powerful face detection technique. In their approach to face detection, Paul Viola and Michael Jones addressed the way in which unnecessary calculation time is not required and are prepared to achieve high precision at the same time.

This approach was proposed in order to introduce a methodology for face recognition that is constantly quicker than other techniques. In recent decades, this approach has been one of the most important and commonly utilised face detection algorithms in real-time applications, owing to its uncompetitive detection speed and reasonably high detection accuracy. Viola and Jones approaches were then used as a primary phase in our model for detecting faces. Phases of facial recognition and normalization detect mask effects and some of the illumination effects are diminished. The next step is the extraction of features, which removes the functionality, and in the collection process no appropriate features are eliminated. The last step is to group the facial expressions into four essential emotions. In general, the facial recognition method utilises two methods, the primary technique depends on face features and the choice takes into consideration the holistic perception of popularity.

2. Literature Review

In recent decades, face recognition has become an interesting area of study. Due to advanced technology of image recognition and neural networks, several researchers have shown interest in this area. In this section, author explain many previous studies on the recognition of expression.

Manjunath and Chellappa [22] suggested a system for the identification of faces using topological graphs that are built from features obtained from Gabor wavelet facial decomposition. This technique decreases storage requirements by preserving the facial features found by decomposition of the Gabor wavelet. The two faces begin with the alignment by matching the centre of the features of those two graphs. This approach therefore has a degree

of robustness in scope, but only in minimal circumstances. In comparison, shifts in illumination and the occluded faces are not considered.

Few versions of the Fisher Linear Discriminator have been developed for FR, such as FD- Linear discriminant analysis, and KDDA (Lu and Plataniotis[23]) etc. However the numerical criteria of these methods are very much linked to the scale of the amount of training samples and initial data. When the face database grows greater, memory, and training time needs may rise dramatically.

Chengjun Liu [21] proposed a novel GFC for FR (face recognition). The Gabor Fisher Classifier process, EFM model refers to the increased Gabor vector generated from the Gabor wavelet representation of face images, which is resilient for shifts in facial expression and illumination . The innovation of their work stems from

1) Derivation of the enhanced Gabor feature vector, which also decreases the dimensionality by Enhanced Fisher linear discriminant Model (, taking both data compression and (generalisation) effects into account;

2) The establishment of a multi-class Gabor-Fisher classification;

3) Comprehensive methods to enhance studies.

Facial expression recognition system is proposed to enhance healthcare services in an extremely smart city. The suggested method uses the transform bandlet [9] on the face picture to remove sub-bands. Each sub-band block by block adds a weighted, CS-LBP pattern. The histograms of the CS-LBP block are merged to provide a vector facial feature. The optional filtering technique extracts the dominant traits, which can then be fed into two categories: GMM and SVM .Until a confidence is made, innumerable of the classificatory are combined by weight to take decisions on the shape of the face. Several experiments are conducted using an oversized data set to validate the proposed process.

A In[17], researchers used stationary wavelet transformation to extract features for the detection of countenances in both spatial domains and spectral . The elimination of functional dimensionality was achieved by the application of a discreet transformation of the cosine. A FNN feed conditioned by a BP algorithm was used as a classification model. The study narrated the emotional processing unit that retrieved the facial activity coding scheme (FACS) and the user's head motion characteristics. The support vector machine[11] has been used as a classification to obtain an accuracy rate of 95.31% for both the motion character face and the head. [7] suggested how facial expressions could be distinguished from a range of poses in the head. The components were mapped using a non-linear form. A hybrid system for automatic countenance recognition has been suggested in[8]. It used HOG descriptor . LDA and PCA were also used as a feature reduction technique.

This paper provides a superior idea for the popularity of human emotions through facial expressions (Frames by frames) employing a Convolution Neural Network (CNN) [16] and the way the thought process of human changes. During this work frame ensemble of classifiers are wont to classify the various emotions from the video sequence. The Gabor wavelet is employed for the temporal feature (Gabor features) extraction of eye and mouth and z-score normalization is applied to get the feature vector. Finally from the obtained Gabor features the universal emotions are classified accordingly.

I[10]In the first instance, the proposed approach builds a data-adaptive graph and sparse with a non-negative constraint. DSLFDA then reproduces the target function as a problem for maximising regression sort. The problem

under sampling is naturally avoided and the slick solution is therefore always reached by applying a ℓ1 penalty to the regression form problem. To prove the feasibility of the proposed procedure, tests on CMU PIE, ORL, and ORL face data databases are performed. It combines not only the idea of LPP in order to preserve the local structure of high-dimensional data, but also FDA in order to achieve discrimination.

Depicts an operation of Multi Support Vector Machine (SVM) [11] with the Convolutional Neural Networks (CNN) [16] [12]. Initially, the characteristics of the pre-processed face image are efficiently extracted by using Local Binary Pattern (LBP), and grey Level Occurrence Matrix (GLCM) and Principal Component Analysis (PCA) . During this model, CNN works as a trainable feature extractor, and Multi-SVM performs as a recognizer.

3. Proposed Process of Present Study

This paper provides a completely unique local descriptor for countenance detection, CS-LOP. In addition to looking at the difference between the grey value of the centre pixel and the surrounding pixels in a total of eight directions, a CS-LOP operator compares the grey value of 4 central-symmetrical pixel pairs. In addition, this study used the CS-LOP The gradient mapping function and, consequently, the Gabor features map are more abundant, detailed, and also extracted features to extract multiple aspects through preprocessed facial image. In figure 1 block diagram of proposed process explained step by step.

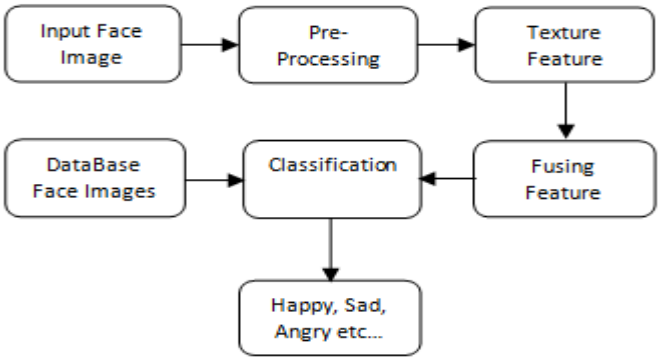

Figure 1: Proposed System

Process/ Flow Diagram

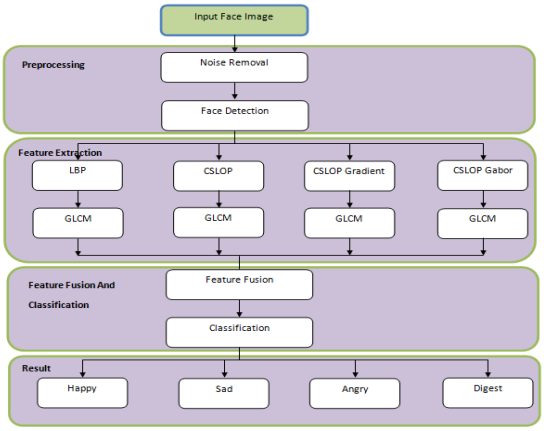

Figure 2: Flow Diagram

In figure 2 flowchart of proposed system has been shown. The detailed explanation is going to be discussed in below sections.

3.1. Preprocessing

The median filter is a digital, non-linear filtering method, sometimes used to eliminate noise from a signal or image. Such a decrease in noise is a standard pre-processing phase to enhance after-treatment performance. The key principle of the middle filter is to join the signal and substitute each input with the median of neighboring entries. The neighbour pattern is called the "window" that slides across the whole signal, input by entry. Median filter tend to minimise random noise, especially if there are broad thresholds and normal trends on the likelihood of noise intensity. The median filtering method is performed by gliding the picture through a glass. The filtered image is generated by putting the median of the values at the center of the picture in the input window.

3.2. Face Detection

Viola-Jones has been built for frontal faces, because it is capable of finding the right face on the front rather than gazing up or down sideways. The picture is transformed into a grey scale until a face is found because work is faster and the data is less processable. The algorithm for the Viola-Jones senses the face of the grayscale picture before finding its place on the coloured image.

Viola-Jones outlines a box and scans for a face in the box (as you can see right). Essentially, it scans for certain haar-like characteristics, which will be clarified later. After crossing each tile in the image, the box shifts a step to the right. Present study used a big box size and did excellent presentation moves, but usually the box size and phase size may be adjusted in compliance with the specifications. A collection of boxes detect facial characteristics with smaller measures (haar-like functionality).

3.3. Haar-like Features

Haar-like structures are the optical image attributes used to identify artifacts. Haar-like feature recognizes a specific location in the recognizing window in adjacent rectangular area, summarizes the pixel intensity in those areas and tests the distance b/w them. This differentiation will then be used to categorize the subsections of the graphic. The identification method would be much more successful if it concentrates on identifying features which encrypt all of

the class information to be recognized. This is the case for Haar-like features that encompass the existence of guided contrasts in the image b/w regions. A selection of these attributes may be used to encode the contrasts between the human facial relationship and face. In the detection process, the goal size window is shifted over the input picture and the HAAR-like feature is measured for each subsection of the image. This disparity is then correlated with the threshold learned, which differentiates non-objects from objects. Since a HAAR -like function is just a weak classifier or learner (its detective efficacy is slightly higher than randoms deviation), it is important to identify an object with sufficient accuracy through a large number of HAAR -like features. Hair-like features are then clustered into something called a cascade classifier to form a strong classifier or learner . The major advantage of the Haar feature over most other characteristics is its calculating speed. Due to the use of integral photographs, a hair function of any type may be continuously calculated. In addition, when the images are examined, each element has its own meaning. It's simple to calculate: deduct the white region from the black one (approximately 60 microprocessor instructions for a 2 feature).

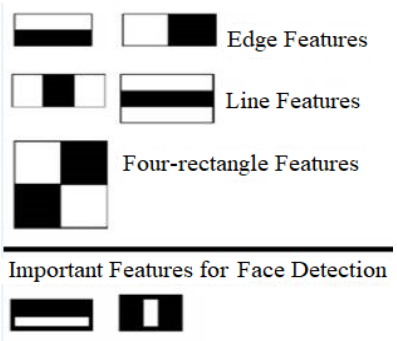

Figure 3: HAAR like feature extraction.

3.4. Local Binary Pattern

The development of the Local Binary Pattern (LBP)[24] is an essential and relevant feature of texture research. The LBP operator and its methodology have inspired and drawn many researchers because the LBP is an effective and unifying solution relative to the typically divergent structural and mathematical models of texture analysis. The LBP has a local property and the methods based on LBP are simple, and this is another explanation that many researchers have focused and applied different methods based on LBP, and these methods have outperformed earlier methods. LBP has a high tolerance for improvements in lighting that have been preferred in real-world implementations. Another significant consideration for LBP is its computational simplicity.

The local binary pattern (LBP) operator is extracted from a large description of texture in the local neighborhood [24] and is a grayscale invariant texture measure. The LBP operator generates a binary code of either 1 or 0 for each pixel in the picture region by fixing its grey value at the centre pixel value [24]. Subsequently, different variants are extracted for this threshold, such as local mean, global mean, etc., in the literature [25, 26, and 27]. Eight adjacent pixels or a 3 x 3 neighborhood are considered only in the basic or basic variant of the LBP operator. This description was later expanded to include all circular neighborhoods of any amount of pixels [24].Mathematically Local Binary Pattern encoded in equation 1 and 2.

$$LBP_{N,R}(C) = \sum_{i=0}^{N-1} s(P_i - P_c)2^i \ldots .1$$

$$P(x) = \begin{cases} 1, & y \geq 0 \\ 0, & y < 0 \end{cases} \ldots\ldots 2$$

Here Pc shows the central pixel's gray value, $Pi = (i = 0, 1 \ldots N - 1)$ = the neighboring pixel's gray value centered at c, $N\ represent$ total number, R the neighborhood's distance.

3.5. Central Symmetric Local Binary Pattern

The present study extracts a function for each pixel in the area using the (CS-LBP) operator that was influenced by LBP. The LBP operator generates very long histograms and is therefore challenging to use in the descriptor area. The LBP operator generates very long histograms & thus is challenging to use in the descriptor area. To create more simple binary patterns, we're just comparing center-symmetric pixel pairs, see fig below. We can see that LBP produces 256 different binary patterns for 8 neighbors, but this is just 16 for CS-LBP. In addition, the robustness of flat-image regions is reached by restricting small-value gray-level variations. Mathematically Central Symmetric Local Binary Pattern(CSLBP) encoded in equation3 and 4.

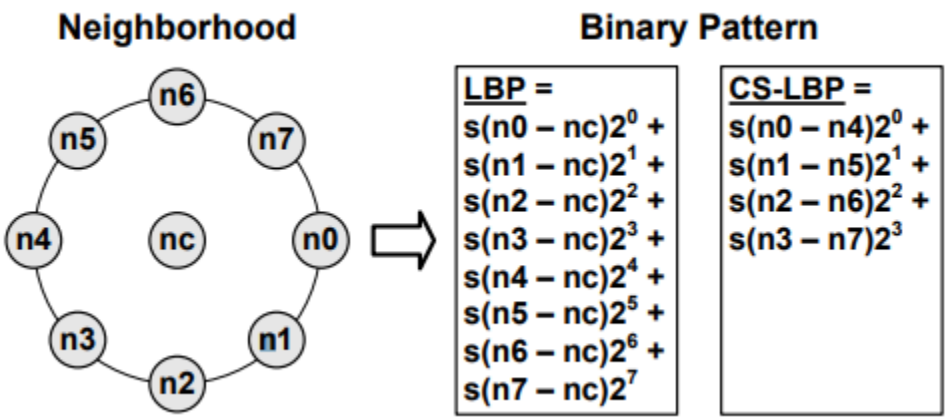

Figure 4: Description of CS-LBP

$$CS - LBP_{N,R}(C) = \sum_{i=0}^{\left(\frac{N}{2}\right)-1} S(P_i - P_{i+\left(\frac{N}{2}\right)})2^i \ldots. (3)$$

$$S(x) = \begin{cases} 1, & y \geq T \\ 0, & y < T \end{cases} \ldots.. (4)$$

Here Pc shows the central pixel's gray value, $Pi\ (i = 0, 1 \ldots N - 1)$ is the neighboring pixel's gray value centered at c, and $N\ represents$ the total number of neighbors concerned. $T\ represent$ experimental threshold and R represent the radius.

3.6. Center-Symmetric Local Octonary Pattern (CS-LOP)

Taking into consideration the LBP operator explained in section II, the contrast of the grey values between the central pixels and the pixels around them is regarded alone however the central symmetrical pair discrepancy is not

complied with. In addition, CS-LBP reduces the size of the vector feature and simplifies the computing sophistication of the LBP idea. The CS-LBP doesn't really take into consideration the core pixels and therefore the threshold (T) has a major effect on the experimental performance. Inspired by the two features mentioned above, this analysis introduces a new descriptor: the (CS-LOP) (CS-LOP).In contrast to matching the grey value of the central pixels with the adjacent pixels, CS-LOP often takes into consideration the grey value of the symmetrical centre of the adjacent pixels so that the texture attributes are more detailed and reliable. Encoding of the CS-LOP is seen in formula described in following equations.

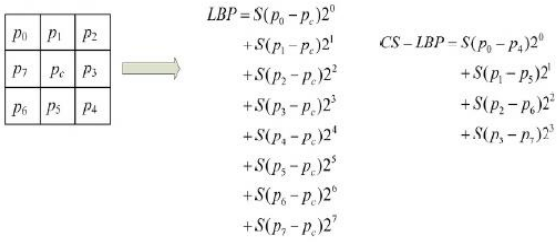

Figure 5: CS-LBP and LBP operators with an eight-pixel neighbour

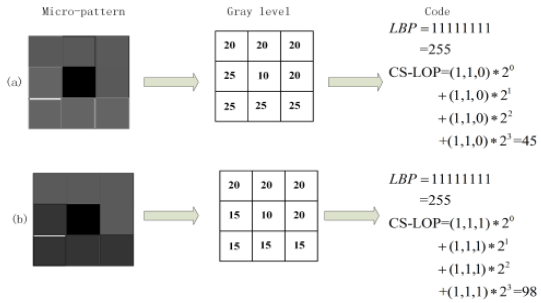

Figure 6: Various micro-patterns with CS-LOP code and LBP code.

$$CS\ LOP_{N,R}(C) = \sum_{i=0}^{\left(\frac{N}{2}\right)-1} \mu(s(Pi - Pc), s(P_{i+\left(\frac{N}{2}\right)} - Pc), \quad s(Pi - P_{(i+\left(\frac{N}{2}\right))})2\text{^}i \quad .. (5)$$

$$s(x) = \{0,\ x < 0\ 1,\ x \geq 0 \quad \ldots (6)$$

$$\mu(a, b, c) = a * 2\text{^}0 + b * 2\text{^}1 + c * 2\text{^}2 \quad ..... (7)$$

In the above equations, N means the cumulative no. of neighbors concerned. P_c is that the central pixel's gray value, $Pi\ (i = 0, 1, \ldots, ((N/2) - 1))$ relates to neighboring pixel's grey value. R is the radius. Present study utilises (a, b, c) for primary period. CS-LOP introduces a single code that converts the value into interval[0, 7], allowing coded values more catching, and diverse the delicate shift of the characteristics b/w pixels so that derived features are more trustworthy or precise. The CS-LBP and LBP operator encodes the result as binary integer, and maps a 4-digit decimal number from 0 to 3. The implementation efficiency of the LBP and CS-LOP is seen in Figure 4.

The two micro-patterns shown in Figures 5 and 6 are quite close from the visual point of view. The created Local Binary Pattern codes are therefore identical. But, CS-LOP operation creates different code values when a center-

symmetric pair of pixels is contrasted by the CS-LOP operator in four directions. The local textures descriptor: CS-LOP has been demonstrated to grab delicate variations within the code values and to reflect non-evident areas.

3.7. Feature Map of Gradient Magnitude Supported By CS-LOP

FMGM is generated using gradient magnitude characteristics to extract texture on a sample of pictures. The expression of gradient scale is centered on the HOG, which corresponds to the vertical and horizontal directions of 4 adjacent pixels, and creates the related gradient meaning, by its size [15]. It is mentioned in equation (8) and (9).

$$G_x(c) = p3 - p4$$

$$G_y(c) = p1 - p5 \quad \ldots (8)$$

$$M(C) = \sqrt{G_x(C)^2 + G_y(C)^2} \quad \ldots. (9)$$

As is being shown in Figure one, $c\ is\ the\ central\ pixel\ of\ the\ 3x3\ rectangle\ area$, p1; p3; p5; p7 are 4 adjacent pixels centered on c. M(c) is the magnitude of the gradient of the c pixel. Gx (c) is the horizontal gradient and Gy(c) is the vertical gradient. After creating gradient maps with an above approach, the CS-LOP is used to extract texture characteristics from the gradient map and gain the characteristic CS-LOP_{FMGM}. With the application of the magnitude gradient, the extracted characteristics are completed.

3.8. Gabor feature chart based on CS-LOP

Gabor wavelet [18] may be a possibly the best descriptor that represents texture features and is almost like the stimulation of simple cells inside the human sensory system. It offers good selection of identity and scale characteristics. The kernel function of the Gabor wavelet is similar to the 2-D area of projection of the cerebral mantle straight cells. It encodes distinct spatial information on intensity, image orientation, position, and extracts subtle local transformations effectively. In addition, the Gabor wavelet is powerful and adapts well to changes in illumination. The kernel function is explained by the Equation (10).

$$G_{\mu,v}(z) = (f(z)) * \varphi_{\mu,v}(z) \quad \ldots\ldots. (10)$$

Where; z describes the pixel's spatial coordinate; v shows Gabor's kernel orientation and scope; may be a regular descriptor; the Gaussian function radius is defined by the parameter. Where * denotes a convolution process, for a filter with 8 directions and 5 scales., {0; 1; 2; : : : ; 7} , v {0; 1; 2; 3; 4} and G;v(z) may be Gabor features's norm .

4. Feature Extractions and Classification

4.1. Texture Feature

A texture that is rough to the touch is distinguished by a broad distance between high and low points and a region between high and low, about the same size as a finger. Picture texture functions exactly the same manner, only that the light values (also called Gray Levels, GL, or Digital Numbers, DN) are high and low rather than elevation shifts. Instead of scanning a finger across the surface, a "window"-a (usually square) box specifying the measurements of the probe-is used.

4.2. Grey-Level Co-Occurrence Matrix

GLCM is a relative frequency square matrix, with two opposite pixels divided by distance d at orientation, one at grey level i and the other at grey level j. This is a test of picture homogeneity that can be determined from the uniform COM. It is a suitable measure for disorder identification in the texture image. Higher values imply fewer shifts in the magnitude or volume of the picture result in a sparser COM. By the subsequent calculation the energy is formulated. The system first selects a seed dot, and then transforms the identical pixels around the seed pixel into seed field. It is used in medical picture segmentation. Particularly for a limited segmentation framework, this is easy.

The Grey-Level Co-occurrence matrix is calculated by Gray-co-matrix from a scaled version of the image. By contrast, graycomatrix scales the picture to 2 gray levels if I is a binary picture. When I an image of intensity, graycomatrix scales the picture to a total of 8 gray-levels. You will set how many gray-levels graycomatrix uses to scale the picture with the parameter 'Number-levels' and how gray-comatrix scales the values using the parameter 'Gray-limit.'

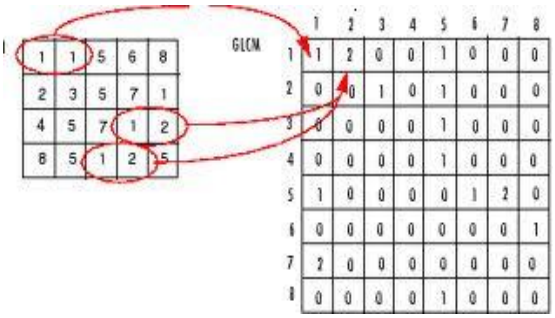

Figure 7: GLCM

4.3. Feature Fusion

A mathematical approach for analyzing the texture considering the pixel spatial associations is GLCM, also known as the gray-level spatial dependency matrix. GLCM functions define the texture of an image by calculating how much in an image, GLCM produces and extracts statistical measurements from the matrix, pixel pairs of individual values and in a precise spatial relationship are located. After you have generated GLCMs using Graycomatrix, you can draw a variety of statistics from them using Graycoprops. These figures provide details on the texture of the image.

The experimental findings demonstrate that LBP, CS-LOP cascades CS-LOP$_{FMGM}$ with a weight then CS-LOP$_{Gabor}$ fuses are capable of achieving the simplest effect.

4.4. Classification

By finishing the supported neural networks, identifying the countenance group . The behavior of biological neurons assisted these statistical models openly.

One of the good accomplishments in the 20th century was the choice of the word "Neural Network." It certainly sounds more fascinating than a technical concept such as a "Network of Nonlinear Transmission Network Weighted Additive Values." Neural networks, for the sake of the term, are far from the use of "thinking machines" or "artificial brains.." In comparison, about 3x1010 neurons are believed to be present in the human nervous system.

Probabilistic Neural Networks (PNN):

PNN and GRNN networks comprise similar architectures, but the fundamental distinction is that they conduct a category of probabilistic networks in which the goal variable is continuous while generalized networks of neuronal regression respond with a constant target. When selecting a Probabilistic Neural Networks/General Regression Neural Network, DTREG automatically selects the correct kind of network that can accommodate the target variable.

OUTPUT = f $[\sum Wo * Ii]$ + BIAS ……(11)

Where W_o is Weight I_i is Input and BIAS is named activation function.

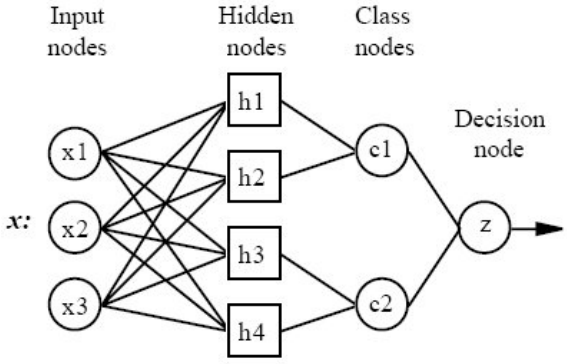

Figure 8: Architecture of a PNN

There are four levels across all PNN networks:

Input layer — For each portion, there is a neuron throughout the input layer. N-1 neurons form the classification variables, where N represents the number of the group. Input neurons are subtracted by standardizing the spectrum of values by the average and inter-quartile distribution (or the processing before the input layer). The input neurons then feed the values to each neuron in the hidden layer.

Hidden layer – for any case in the training data collection, this layer has one neuron. The neuron stores the predictor values alongside the goal value of the event. A secret neuron measures the Euclidean distance from the centre point of the neuron, then the RBF kernel function applies the sigma value if the x vector of input values is reflected in the input level (s). In the pattern layer, the consequent meaning is transferred to the neurons.

Summation layer/ Pattern layer — the network layer is separate from the network for PNN and GRNN networks. Pattern layer for each type of the goal variable, there is one sequence neuron for PNN networks. Per hidden neuron has its own target category; only the pattern neuron that fits the category of the hidden neuron is fed to the weighted start value of the hidden neuron. The neurons of the pattern apply the values for their respective category (thus, for that division it is a weighted vote).

Just two neurons in the pattern layer occur for GRNN networks. One neuron is that the summing unit of the denominator is the summing unit of the numerator. The Summing unit of the denominator adds the load values of each neuron. The Summing Unit for the Numberator adds the load values multiplied by each secret neurons aim.

Decision layer — For PNN and GRNN networks, the choosing layer is distinct. For PNN networks the selection layer uses the most relevant vote to predict the goal category to compares the weighted votes for each aim category accumulating inside the pattern layer.

In the case of General Regression Neural Network networks the value accrued by the value is divided inside the numerator overview unit and the outcome is used since the goal value is expected.PNN are a kind of radial basis network suitable for classification problems.

Net = Probabilistic Neural Networks (P, T, spread) accumulate 2 or 3 arguments,

- P to R-with Q input vector's Q matrix.
- T to S-with- Q target class vector's Q matrix.
- Spread to spread of radial basis functions.

Neural network generates a network of two layers. The first layer has radbas neurons and the weighted inputs on dist and netprod are computed. The 2nd layer has opposing neurons and its weighted income is measured with dotprod and netsum. Only the first layer is incomplete. We could determine facial expression on the basis of the net.

- 1 - Normal
- 2- Smile
- 3-Surprise
- 4-Sad
- 5-Disgus
- 6-Not available

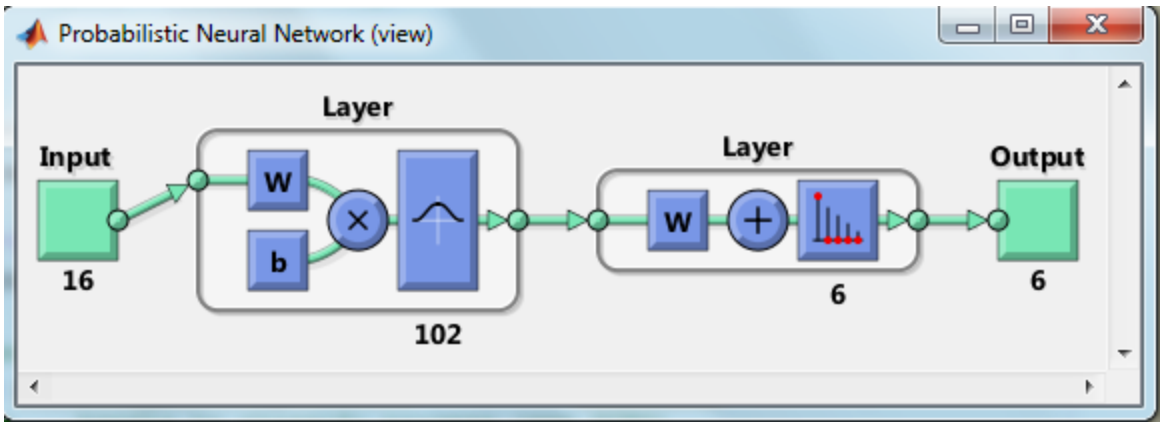

Figure 9: Description of PNN structure.

5. Results and Discussion

Algorithms are included in this segment to validate the utility of the proposed methods for facial expression recognition. The usage of MATLAB 2013b has been carried out for all studies

A. Construction of Dataset

Two prominent facial picture sets were used to test the proposed algorithm: JAFFE Archive of the 10 female designers of the Japanese model includes 213 pictures of 7 facial expressions (6 fundamental facial expressions + 1 neutral).

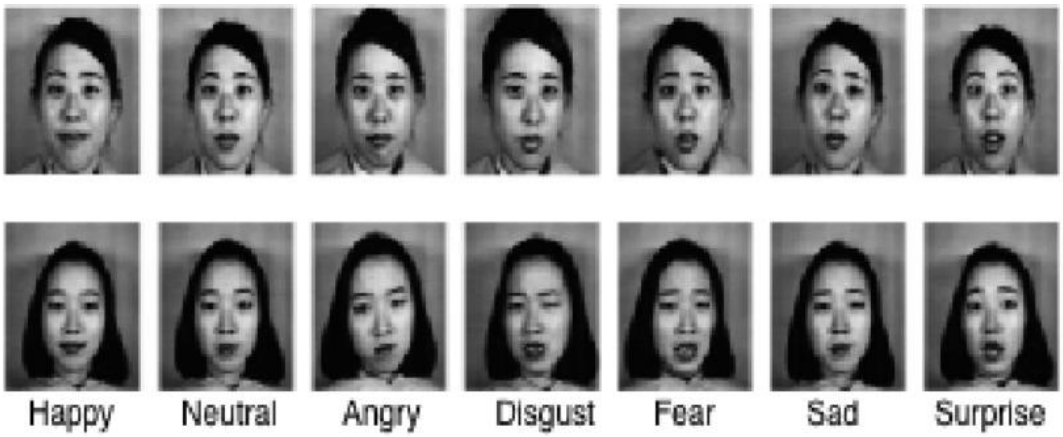

Examples of JAFFE facial expression

Figure 4 provides one example of the terminology for the two data sets (from right to left, expressions are ; surprise, sad, fear, disgust, angry, Neutral, happy,). Three photos of each speech in JAFFE with 7 facial expressions are chosen in our experiments .Six fundamental facial gestures and one facial neutral.

B. Steps of Experiment

1) PREPROCESS:

Pre-processing of images can be split down into three steps:

(a) Detect human eyes with the Jones Algorithm, and use two-eye coordinates to remove pose impact from the picture Haar features.

(b) Image scale detection and cut to (256X256);

(c) Image filter image processing is used to eliminate noise from the Gaussian filter in order to minimize the influence of noise and increase recognition performance [28].

2) Fusion and Feature Extraction

This study uses the CS-LOP descriptor to remove structure features from the pre-processed visual image, feature graphic charts, maps of Gabor, and then three characteristics: LBP,CS-LOP,CS-LOP$_{Gabor}$. The extraction method; LBP, CS-LOP, CS-LOP$_{Gabor}$ and the fused procedure is carried out on JAFFE.

3) Classification

The identification of face speech groups through the use of PNN is a form of radial base network ideal for classification issues.

C. Experimental Results and Analysis

Algorithms are included in this segment to validate the utility of the proposed methods for facial expression recognition. The usage of MATLAB 2013b has been carried out for all studies (ref figure 10a, 10b and 10c).

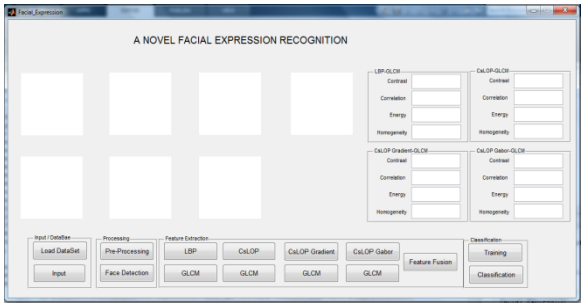

Figure 10a: Main window for step by step process.

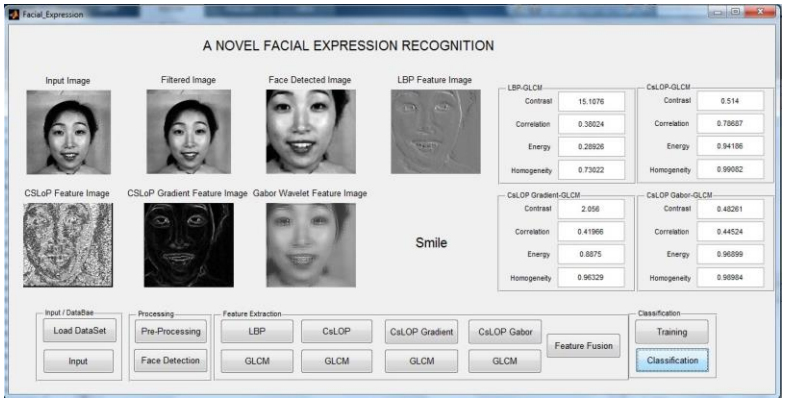

Figure 10(b) Recognition of smiles

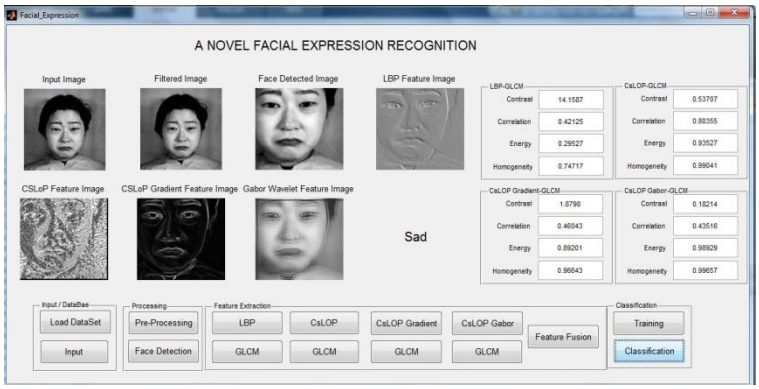

Figure 10 (c) Recognition of sad

The five-sized and eight-oriented Gabor filter is used to transform images, and Forty Gabor feature maps are generated per frame. The converted Gabor maps substantially increase the number of test samples and the duration of preparation. The amount of scale channels (μ) used by Gabor filters was evaluated in this study with a view to

minimizing time complexity. For the extraction of features, the first 8 μ *sheets* (μ 1, 2, 3, 4, 5) are chosen from the

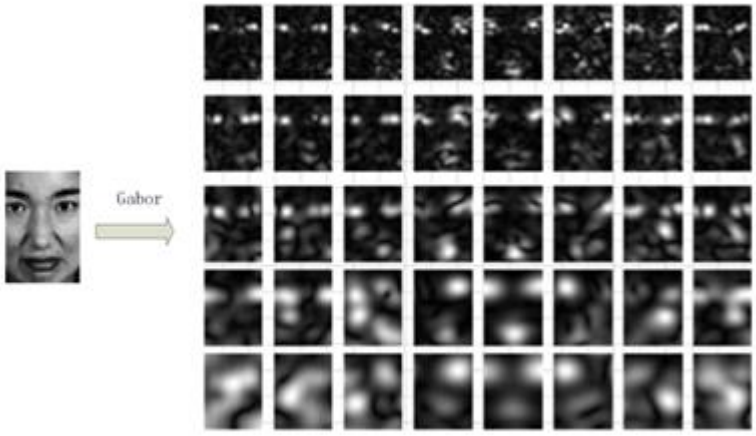

Gabor feature maps.

Figure 11: Map of a facial image of Gabor feature

i) Comparison of the Recognition Rate (RR) (%)

There are four distinct features: LBP, CSLOP, $CSLOP_{Gradient}$ and $CSLOP_{Gabor}$. There is also fused methods for these four approaches which is consist of addition of all(LBP, CSLOP, $CSLOP_{Gradient}$ and $CSLOP_{Gabor}$). The experimental finding suggests that the JAFFE facial expressions of CS-LOP and $CS\text{-}LOP_{FMGM}$ are complementary. Figure 13 has shown different RR for different facial expression.

First LBP,CSLOP, $CSLOP_{Gradient}$ and $CSLOP_{Gabor}$ has been applied and for all these feature and recognition rate are 84.97 % ,97.24%, 97.83% and 97.65 % respectively. At last fused method is applied to improve performance of recognition rate (RR) which gives 98.69% RR as shown in table 1.

Table 1: Recognition rate for different features

Method	JAFFE
LBP	84.41 %
CSLOP	97.24 %
CSLOP_Gradient	97.83 %
CSLOP Gabor	97.65 %
Fused Method	98.69 %

ii) Comparison of Accuracy (%) for Different Approaches

In relation, our fused approach is compared with other single facial expression recognition methods and comparison findings in Table 2 to further show the reasonability of over all of the algorithms. Here present study approaches six algorithms in which accuracy rates of (Image pyramid +decision tree) ,LDTP, Local Curvelet transform ,Features Co Clustering ,Deep CNN ,(LBP+LPQ + Gabor) and Fused method are 91.43% 93.2%,94.65% 96.25% ,97.715 ,98.57 % and 99.45% respectively. Graphically representation of accuracy (%) comparison for different facial expression are shown in figure 12.. The following table shows that the approach proposed works not only better than the traditional characteristic descriptors but also better than the rest to certain methods by using DNN. To conclude, its superiority and excellence in facial recognition is demonstrated by the proposed operator CS-LOP and its fusion methods.

Table 2: Accuracy (percent) comparison of various methods of recognition of facial expression

Method	JAFFE
Image Pyramid + decision tree	91.43
LDTP	93.2
Local Curvelet Transform	94.65
Feature Co Clustering	96.25
Deep CNN	97.71
LBP + LPQ + Gabor	98.57
Fused Method	99.45

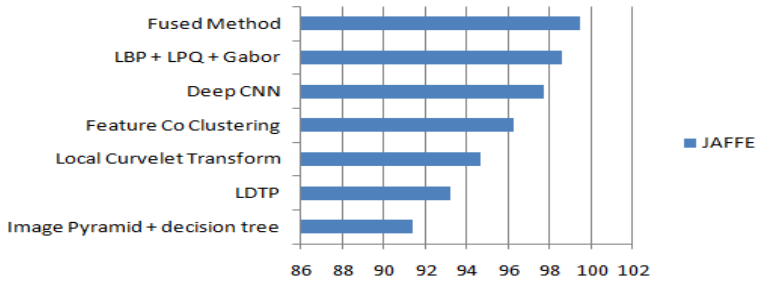

Figure 12: Accuracy (%) comparison of different facial expression

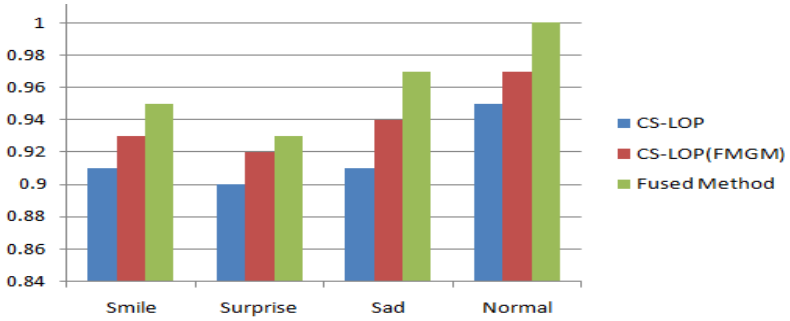

Figure 13: the Recognition rate of different expressions in JAFFE

6. Conclusion

In this article, the grey value of central-symmetric four-pixel pairs is not only compared with neighboring-bound pixels in all 8 directions, often measures the gray value of 4 sets of center-symmetric pixels. We have uses LBP, CSLOP, $CSLOP_{Gradient}$ and $CSLOP_{Gabor}$ for feature extraction process. Here we found that LBP has minimum

recognition rate of 84.41% and fused method which consist of adding all the GLCM of LBP, CSLOP, CS-LOP$_{gradient}$, CSLOP Gabor has maximum recognition rate. In this process CS-LOP bring down the vector dimension of the feature relied on Local Binary Pattern (LBP) and prevents optimization of the threshold. The addition of one bit code value added by the CS-LOP operator allows acute and detailed pixels of unexpected areas to capture and represent compared to pre-historic descriptors, such as the following: Local Binary Pattern (LBP) and CS- Local Binary Pattern(CSLOP) coding. CS-LOP operator later to remove features on the facial picture, the gradient map and the Gabor mapping feature, and then to fuse the three features for facial expression recognitions to the corresponding CS-LOP, CS-LOP$_{gradient}$ and CS-LOP$_{Gabor}$. This study analyze the formulation of the proposed algorithm and the research findings of JAFFE data sets show that the CS-LOP performs better than other characteristics and enhance the efficiency of as a whole recognition compared with state-of-the-art methods. At last we have compared the accuracy percentage of different recognition methods and we found that image pyramid and decision tree has minimum accuracy rate of 91.43 and present study purposed method has 99.45% of accuracy rate. All of this research demonstrates that not only does the proposed method perform better than certain traditional descriptors of characteristics, but it is also similar to other methods that use DNN. In summary, their supremacy and competence in face gestures are shown by the suggested CS-LOP operator and their composite methods.

Future scope:

We have taken the JAFFE data collection, which limits existing research to unique face character characters (Japanese). In the future, we can conduct this fused analysis on various data sets to analyze the recognition rate for different facial expressions.

REFERENCE

[1] D. Kim, *Automated Face Analysis: Emerging Technologies and Research*. Pennsylvania, PA, USA: IGI Global, 2009.

[2] M. Z. Uddin, M. M. Hassan, A. Almogren, A. Alamri, M. Alrubaian, and G. Fortino, ``Facial expression recognition utilizing local direction based robust features and deep belief network," *IEEE Access*, vol. 5, pp. 4525_4536, 2017.

[3] F. Ren and Z. Huang, ``Automatic facial expression learning method based on humanoid robot XIN-REN," *IEEE Trans. Human-Mach. Syst.*, vol. 46, no. 6, pp. 810_821, Dec. 2016.

[4] P. Ekman andW. V. Friesen, *Unmasking the Face: A Guide to Recognizing Emotions From Facial Expressions*. California, CA, USA: Ishk, 2003.

[5] F. De la Torre and J. F. Cohn, ``Facial expression analysis," *Visual Analysis of Humans*. London, U.K.: Springer, 2011, pp. 377_409.

[6] F. Ren andY.Wu, ``Predicting user-topic opinions in twitter with social and topical context," *IEEE Trans. Affective Comput.*, vol. 4, no. 4, pp. 412_424, Oct./Dec. 2013.

[7] M. Jampour, V. Lepetit, T. Mauthner, and H. Bischof, ``Pose-speci_c non-linear mappings in feature space towards multiview facial expression recognition," *Image Vis. Comput.*, vol. 58, pp. 38_46, Feb. 2017.

[8] N. B. Kar, K. S. Babu, and S. K. Jena, ``Face expression recognition using histograms of oriented gradients with reduced features," in *Proc. Int. Conf. Comput. Vis. Image Process. (CVIP)*, vol. 2. 2016, pp. 209_219, 2017.

[9] Muhammad, Mansour Alsulaiman, Syed Umar Amin, Ahmed Ghoneim, And Mohammed F. Alhamid, ``A Facial-Expression Monitoring System for Improved Healthcare in Smart Cities GHULAM" *IEE Acess. J.*, vol. 5, pp. 10871-10881, May 28. 2017.

[10] Zhan Wang, Qiuqi Ruan, and Gaoyun An, ``Face Recognition Using Double Sparse Local Fisher Discriminant Analysis" Hindawi Publishing Corporation, Article *in* Mathematical Problems in Engineering · March 2015 DOI: 10.1155/2015/636928

[11] Chamasemani, F. F., & Singh, Y. P. (2011, September). Multi-class support vector machine (SVM) classifiers--an application in hypothyroid detection and classification. In *Bio-Inspired Computing: Theories and Applications (BIC-TA), 2011 Sixth International Conference on* (pp. 351-356).

[12] Lopes, A. T., de Aguiar, E., De Souza, A. F., & Oliveira-Santos, T. (2017). Facial expression recognition with convolutional neural networks: coping with few data and the training sample order. Pattern Recognition, 61, 610-628.

[13] T. Ojala, M. Pietikäinen, and T. Maenpaa, ``Multiresolution gray-scale and rotation invariant texture classi_cation with local binary patterns," *IEEE Trans. Pattern Anal. Mach. Intell.*, vol. 24, no. 7, pp. 971_987, Jul. 2002.

[14] M. Heikkilä, M. Pietikäinen, and C. Schmid, ``Description of interest regions with local binary patterns," *Pattern Recognit.*, vol. 42, no. 3, pp. 425_436, 2009.

[15] N.-S. Vu and A. Caplier, ``Face recognition with patterns of oriented edge magnitudes," in *Proc. Eur. Conf. Comput. Vis.* Berlin, Germany: Springer, 2010, pp. 313_326.

[16] Pons, G., &Masip, D. (2017). Supervised Committee of Convolutional Neural Networks in Automated Facial Expression Analysis. IEEE Transactions on Affective Computing.

[17] H. Qayyum, M. Majid, S. M. Anwar, and B. Khan, ``Facial expression recognition using stationary wavelet transform features," *Math. Problems Eng.*, vol. 2017, 2017, Art. no. 9854050.

[18] B. Zhang, G. Liu, and G. Xie, ``Facial expression recognition using LBP and LPQ based on Gabor wavelet transform," in *Proc. 2nd IEEE Int. Conf. Comput. Commun. (ICCC)*, Oct. 2016, pp. 365_369.

[19] G. Muhammad, M. Alsulaiman, S. U. Amin, A. Ghoneim, and M. F. Alhamid, ``A facial-expression monitoring system for improved healthcare in smart cities," *IEEE Access*, vol. 5, pp. 10871_10881, 2017.

[20] X. Zhu and D. Ramanan, "Face detection, pose estimation, and landmark localization in the wild," in *Proc. IEEE Conf. Comput. Vis. Pattern Recognit.*, Jun. 2012, pp. 2879–2886.

[21] Liu, C. and Wechsler, H., 2002. Gabor feature based classification using the enhanced fisher linear discriminant model for face recognition. *IEEE Transactions on Image processing*, *11*(4), pp.467-476.

[22] Chellappa, R., Manjunath, B.S. and Malsburg, C.V.D., 1992. A feature based approach to face recognition. In *IEEE Conference on Computer Vision and Pattern Recognition* (pp. 373-378).

[23]Juwei Lu, Plataniotis K.N. and Venetsanopoulos A.N. (2003), 'Face recognition using LDA based algorithms', IEEE Transactions on Neural Networks, Vol. 14, No. 1, pp. 195-200.

[24] T.Ojala, T.Maenpaa and M.Pietikainen. Gray scale and rotation invariant texture classification with local binary pattern, Computer Vision, Springer, (2000) 404-420.

[25] H.Jin, H.Lu and X.Tong, Face detection using improved local binary pattern under Bayesian framework, Multi Agent Security and Survivability, IEEE Symposium, (2004) 306-309.

[26] A.Hafiane, G.Seetaraaman, Median binary pattern for textures classification, Springer, Image Analysis and Recognition, (2007) 387-398.

[27] B.Froba and A.Ernest, Face detection with the modified census transform, Automated Face and Gesture Recognition, IEEE Conf., (2004) 91-96.

[28] J. P. Jones and L. A. Palmer, ‘‘An evaluation of the two-dimensional Gabor filter model of simple receptive fields in cat striate cortex,’’ *J. Neurophys- iol.*, vol. 58, no. 6, pp. 1233–1258, Dec. 1987.